

Characterizing the spin orbit torque field-like term in in-plane magnetic system using transverse field

Feilong Luo, Sarjoosing Goolaup, Sihua Li, Gerard Joseph Lim, Funan Tan, Christian Engel, Senfu Zhang, Fusheng Ma, Tiejun Zhou, and Wen Siang Lew

Citation: *Journal of Applied Physics* **120**, 083908 (2016); doi: 10.1063/1.4961952

View online: <http://dx.doi.org/10.1063/1.4961952>

View Table of Contents: <http://scitation.aip.org/content/aip/journal/jap/120/8?ver=pdfcov>

Published by the [AIP Publishing](#)

Articles you may be interested in

[In-plane current-driven spin-orbit torque switching in perpendicularly magnetized films with enhanced thermal tolerance](#)

Appl. Phys. Lett. **108**, 212406 (2016); 10.1063/1.4952771

[Engineering spin-orbit torque in Co/Pt multilayers with perpendicular magnetic anisotropy](#)

Appl. Phys. Lett. **107**, 232407 (2015); 10.1063/1.4937443

[Landau-Lifshitz equations and spin dynamics in a heterostructure with a broken inversion symmetry, under spin-orbit torque transfer of the spin moment](#)

Low Temp. Phys. **41**, 689 (2015); 10.1063/1.4931647

[Enhanced spin-orbit torques in Pt/Co/Ta heterostructures](#)

Appl. Phys. Lett. **105**, 212404 (2014); 10.1063/1.4902529

[Linear magnetic field response spin valve with perpendicular anisotropy ferromagnet layer](#)

J. Appl. Phys. **103**, 07E906 (2008); 10.1063/1.2830968

A promotional banner for AIP Applied Physics Reviews. The background is a dark blue gradient with a bright light source on the right, creating a lens flare effect. On the left, there is a small image of the journal cover for 'Applied Physics Reviews', which features a 3D diagram of a layered structure. The main text 'NEW Special Topic Sections' is written in large, white, sans-serif font. Below this, the text 'NOW ONLINE' is in yellow, followed by 'Lithium Niobate Properties and Applications: Reviews of Emerging Trends' in white. The AIP Applied Physics Reviews logo is in the bottom right corner.

NEW Special Topic Sections

NOW ONLINE
Lithium Niobate Properties and Applications:
Reviews of Emerging Trends

AIP Applied Physics
Reviews

Characterizing the spin orbit torque field-like term in in-plane magnetic system using transverse field

Feilong Luo,^{1,2} Sarjoosing Goolaup,¹ Sihua Li,¹ Gerard Joseph Lim,¹ Funan Tan,¹ Christian Engel,¹ Senfu Zhang,¹ Fusheng Ma,¹ Tiejun Zhou,² and Wen Siang Lew^{1,a)}

¹*School of Physical and Mathematical Sciences, Nanyang Technological University, 21 Nanyang Link, Singapore 637371*

²*Data Storage Institute, (A*STAR) Agency for Science, Technology and Research, DSI Building, 5 Engineering Drive 1, Singapore 117608*

(Received 8 April 2016; accepted 18 August 2016; published online 31 August 2016)

In this work, we present an efficient method for characterizing the spin orbit torque field-like term in an in-plane magnetized system using the harmonic measurement technique. This method does not require *a priori* knowledge of the planar and anomalous hall resistances and is insensitive to non-uniformity in magnetization, as opposed to the conventional harmonic technique. We theoretically and experimentally demonstrate that the field-like term in the Ta/Co/Pt film stack with in-plane magnetic anisotropy can be obtained by an in-plane transverse field sweep as expected, and magnetization non-uniformity is prevented by the application of fixed magnetic field. The experimental results are in agreement with the analytical calculations. *Published by AIP Publishing.* [<http://dx.doi.org/10.1063/1.4961952>]

I. INTRODUCTION

The controlled displacement of domain walls (DWs) using spin-polarized current has opened up potential for new types of magnetic memory and logic devices.^{1,2} In ferromagnetic materials (FMs), the spin transfer torque (STT) is responsible for the DW motion along the direction of electron flow.³ The direct transfer of the spin angular momentum of electrons to the magnetic moments of the system leads to DW dynamics.⁴ Recently, it has been shown that structures comprising a FM layer with an adjacent heavy metal (HM) layer exhibit DW motion against the direction of electron flow, which can be explained by the spin-orbit torque (SOT) mechanism.^{5–7} This phenomenon in the FM/HM heterostructure is attributed to the spin Hall effect of the HM layers as well as the Rashba effect, which originates from the HM layers and interfaces of the FM/HM.^{5,6,8} The two effects generate two distinct effective SOT fields which influence the magnetization of the FM layer; one is the damping-like term which depends on the magnetization of the magnetic layer and the other is the field-like term which is independent of the magnetization of the magnetic layer.⁹

The detection of the SOT fields in the FM/HM heterostructures can be carried out using the harmonic measurement technique whereby the tilting of the magnetic moments of the FM layer is detected by the Hall measurement.⁹ As the tilting angle of the magnetic moment is directly correlated with the SOT fields, the measurement of the tilting angle provides an estimate of the fields. In the harmonic measurement scheme, an alternating current (AC) is applied to the FM/HM wire and this leads to harmonic voltages which are detected at a Hall cross structure. The first harmonic voltage detects the rotation of magnetization induced by the

externally applied magnetic field, while the second harmonic voltage detects small oscillations of the magnetization induced by SOT fields. This measurement technique has been widely used for the detection of SOT fields in perpendicular magnetic anisotropy (PMA) structures.^{10–12} However, it has been recently reported that SOT fields are more effective for magnetization switching for materials with in-plane magnetic anisotropy (IMA) rather than materials with PMA. This has been attributed to the field-like term contributing towards a significant decrease in the critical current density required for magnetization switching.¹³ Thus, the field-like term which is rarely studied for films with IMA has significant potential for SOT devices.

Hayashi *et al.* reported that the field-like term in the IMA film can be obtained by sweeping a magnetic field which is tilted with respect to the plane of the IMA film.⁹ The perpendicular field component is for measuring the first harmonic voltage from the anomalous Hall effect (AHE). The in-plane field component, which is preferably aligned along the magnetic easy axis, is used to measure the second harmonic voltage from the planar Hall effect (PHE). As such, the AHE and PHE resistances are required for calculating the field-like term. This method relies on a uniform magnetization at the Hall cross. However, a domain wall is likely to be nucleated at the Hall cross when the tilted field is increased. This can result in the second harmonic voltage being zero, hence resulting in a calculated field-like term of zero.

In this work, we show through analytical derivation that the field-like term of the SOT in the IMA system can be obtained by sweeping the field along the same direction of the field-like term, without prior knowledge of the Hall resistances. Uniform magnetization can then be sustained by applying a constant field along the magnetic easy axis. In the experimental verification, a fixed magnetic field is

^{a)}Author to whom correspondence should be addressed. Electronic mail: wensiang@ntu.edu.sg.

applied along the long axis of a Ta/Co/Pt magnetic wire, while sweeping the field transversely to the wire. The experimentally obtained values of the effective fields at different current densities are larger than the calculated Oersted fields. The measurement results are in agreement with our theoretical analysis. The magnitude of the measured field-like term is in the same order as those reported for PMA systems.¹¹

II. THEORY

Figure 1 shows the optical microscopy image of the investigated in-plane magnetized wire and a schematic of the orientation of magnetization, \mathbf{M}_s . The total magnetic energy density of the wire can be written as

$$E = (N_z M_s^2 - K) \sin^2 \theta + N_y M_s^2 \cos^2 \theta \sin^2 \varphi - M_s H_{z-ext} \sin \theta - M_s H_{x-ext} \cos \theta \cos \varphi - M_s H_{y-ext} \cos \theta \sin \varphi, \quad (1)$$

where $N_z M_s^2$ is the perpendicular demagnetizing energy density which is larger than the interface perpendicular anisotropy energy density K in the IMA system,¹³ N_z and N_y are the demagnetizing factors along z and y directions, θ and φ are the elevation and azimuth angles of the magnetization, respectively, and \mathbf{H}_{x-ext} , \mathbf{H}_{y-ext} , and \mathbf{H}_{z-ext} are the applied field components along the three major axes. For small θ , $\cos \theta \approx 1$, Equation (1) can be simplified as

$$E = (N_z M_s^2 - K) \sin^2 \theta + N_y M_s^2 \sin^2 \varphi - M_s H_{z-ext} \sin \theta - M_s H_{x-ext} \cos \varphi - M_s H_{y-ext} \sin \varphi. \quad (2)$$

A stable angle θ_0 can be obtained by the partial derivative of E with respect to θ and equating to 0

$$\frac{\partial E}{\partial \theta} = 2 \left(N_z M_s - \frac{K}{M_s} \right) \sin \theta - H_{z-ext} = 0. \quad (3)$$

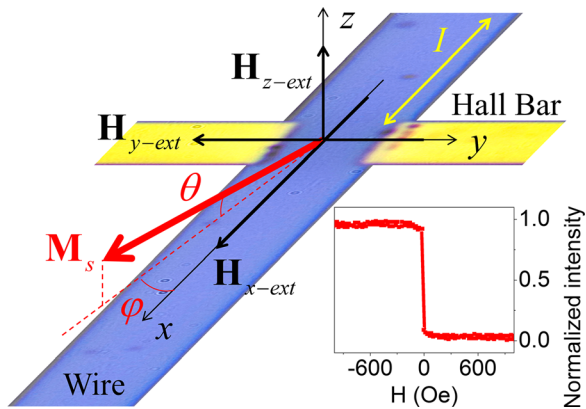


FIG. 1. Optical microscopy image of the investigated in-plane magnetized wire and a schematic of the orientation of magnetization. The magnetic layer has an in-plane easy axis which is along the wire long axis. θ is the elevation angle between the magnetization \mathbf{M}_s and the plane of thin film, and φ is the azimuth angle of \mathbf{M}_s to the easy axis. \mathbf{H}_{x-ext} , \mathbf{H}_{y-ext} , and \mathbf{H}_{z-ext} are the fields applied along three major directions. The inset shows the normalized longitudinal MOKE curve for the thin film Ta(10nm)/Co(2nm)/Pt(5nm).

Solving for θ_0 , we obtain

$$\theta_0 \approx \frac{H_{z-ext}}{2(N_z M_s - K/M_s)} \quad \text{and} \quad \Delta \theta_0 = \frac{1}{2(N_z M_s - K/M_s)} \Delta H_{z-ext}. \quad (4)$$

Similarly, a stable angle φ_0 can be obtained by taking the partial derivative of E with respect to φ and equating to 0

$$\frac{\partial E}{\partial \varphi} = H_{x-ext} \tan \varphi + 2N_y M_s \sin \varphi - H_{y-ext} = 0. \quad (5)$$

For small value of φ , $\tan \varphi$ and $\sin \varphi$ can be approximated to φ . Equation (5) can then be rewritten as

$$\varphi_0 \approx \frac{H_{y-ext}}{H_{x-ext} + 2N_y M_s} \quad \text{and} \quad \Delta \varphi_0 = \frac{1}{H_{x-ext} + 2N_y M_s} \Delta H_{y-ext}. \quad (6)$$

When an alternating electric current, $I = I_0 \sin \omega t$, flows through the wire, the effective fields generated by the current are: field-like term, $H_{y-SOT\&Oe} = H_{0-y-SOT\&Oe} \sin \omega t$, acting transversely to the wire and damping-like term, $H_{z-SOT} = H_{0-z-SOT} \sin \omega t$, which is perpendicular to the plane of the wire.⁹ I_0 and ω are the amplitude and angular frequency of the applied current. The change in the magnetization orientation of the wire, $\Delta \theta_0$ and $\Delta \varphi_0$, induced by H_{z-SOT} and $H_{y-SOT\&Oe}$ can be obtained from Eqs. (4) and (6), respectively. Alternatively,

$$\Delta \theta_0 = \frac{1}{2(N_z M_s - K/M_s)} H_{z-SOT} \quad \text{and} \quad \Delta \varphi_0 = \frac{1}{H_{x-ext} + 2N_y M_s} H_{y-SOT\&Oe}. \quad (7)$$

The angles θ and φ can be written as

$$\theta = \theta_0 + \Delta \theta_0 \quad \text{and} \quad \varphi = \varphi_0 + \Delta \varphi_0. \quad (8)$$

The resulting voltage, V , across the Hall bar generally comprises two components: anomalous Hall effect (AHE) voltage V_a and planar Hall effect (PHE) voltage V_p

$$V = V_a + V_p, \quad (9)$$

where $V_a = I_0 \rho_a \sin \theta \sin \omega t$ and $V_p = I_0 \rho_p \cos^2 \theta \sin 2\varphi \sin \omega t$; ρ_a and ρ_p are the AHE and PHE resistances, respectively.⁹ The ordinary Hall effect is not considered here. Equation (9) can be rewritten by substituting θ and φ from Eq. (8)

$$V = I_0 \rho_a \sin(\theta_0 + \Delta \theta_0) \sin \omega t + I_0 \rho_p \cos^2(\theta_0 + \Delta \theta_0) \sin 2(\varphi_0 + \Delta \varphi_0) \sin \omega t. \quad (10)$$

Since we assume $\cos \theta \approx 1$, Eq. (10) reduces to

$$V \approx I_0 \rho_a [\sin \theta_0 + \Delta \theta_0] \sin \omega t + I_0 \rho_p [\sin 2\varphi_0 + 2\Delta \varphi_0 \cos 2\varphi_0] \sin \omega t, \quad (11)$$

when $\Delta \theta_0$ and $\Delta \varphi_0$ are small. Using the identity $\cos 2\varphi_0 = 1 - 2\sin^2 \varphi_0$ and substituting into Eqs. (4) and (6), Eq. (11) can be written as

$$\begin{aligned}
V = & \frac{I_0 \rho_a H_{z-ext}}{2(N_z M_s - K/M_s)} \sin \omega t - \frac{I_0 \rho_a H_{0-z-SOT}}{2(N_z M_s - K/M_s)} \cos 2\omega t \\
& + \frac{2I_0 \rho_p H_{y-ext}}{H_{x-ext} + 2N_y M_s} \sin \omega t - \frac{2I_0 \rho_p H_{0-y-SOT\&Oe}}{H_{x-ext} + 2N_y M_s} \cos 2\omega t \\
& + \frac{4I_0 \rho_p H_{0-y-SOT\&Oe} H_{y-ext}^2}{(H_{x-ext} + 2N_y M_s)^3} \cos 2\omega t + V_{DC}, \quad (12)
\end{aligned}$$

where V_{DC} is the direct voltage. From Eqs. (11) and (12), $\sin 2\varphi_0$ is approximated to $2\varphi_0$ for simplicity. H_{z-ext} is not applied to avoid the AHE; the first harmonic voltage is given as

$$V_\omega = \frac{2I_0 \rho_p}{H_{x-ext} + 2N_y M_s} H_{y-ext} \sin \omega t, \quad (13)$$

and the second harmonic voltage is

$$V_{2\omega} = \frac{4I_0 \rho_p H_{0-y-SOT\&Oe}}{(H_{x-ext} + 2N_y M_s)^3} H_{y-ext}^2 \cos 2\omega t - A \cos 2\omega t, \quad (14)$$

where $A = \frac{2I_0 \rho_p H_{0-y-SOT\&Oe}}{H_{x-ext} + 2N_y M_s} + \frac{I_0 \rho_a H_{0-z-SOT}}{2(N_z M_s - K/M_s)}$ is independent of the external field H_{y-ext} . Thus, using Eqs. (13) and (14), the effective field $H_{0-y-SOT\&Oe}$ can be obtained by

$$H_{0-y-SOT\&Oe} = \left(\frac{H_{x-ext} + 2N_y M_s}{2} \right)^2 \frac{\partial^2 V_{2\omega}}{\partial H_{y-ext}^2} \bigg/ \frac{\partial V_\omega}{\partial H_{y-ext}}. \quad (15)$$

III. EXPERIMENTS AND DISCUSSION

A. The measurement of harmonic voltages

To measure the field-like term in the IMA system, a thin film stack of Ta(10 nm)/Co(2 nm)/Pt(5 nm) was grown using ultrahigh vacuum magnetron sputtering deposition technique. The longitudinal magnetic optical Kerr effect (MOKE) measurement confirms the in-plane magnetic anisotropy property of the film, as shown in the inset of Fig. 1. The film was patterned into wire using a combination of electron beam lithography (EBL) and ion-milling. A Hall bar structure of Ta(5 nm)/Cu(90 nm)/Au(20 nm) was patterned using EBL and added using the lift-off technique. The harmonic voltages were detected using the lock-in technique. A permanent magnet was used to generate a relatively large field $H_{x-ext} = 1200$ Oe to saturate the magnetization of the wire along the long axis. This ensured a uniform magnetization along the long axis with no formation of magnetic domain walls. Alternating current, with different amplitudes at a fixed frequency of 307.1 Hz, was applied to the wire while the magnetic field was swept in the transverse direction to the long axis of the wire.

In the harmonic measurements, the in-plane transverse field, H_{y-ext} , is swept from -300 Oe to $+300$ Oe. The current density is varied from 1×10^{10} Am $^{-2}$ to 7×10^{10} Am $^{-2}$, to ensure that Joule heating is negligible.¹⁰ The first harmonic voltages as a function of the applied field H_{y-ext} for different current densities are plotted in Fig. 2(a). As expected from Eq. (13), they are linear to the externally applied field H_{y-ext} . We note that the $\frac{\partial V_\omega}{\partial H_{y-ext}}$ increases with increasing current

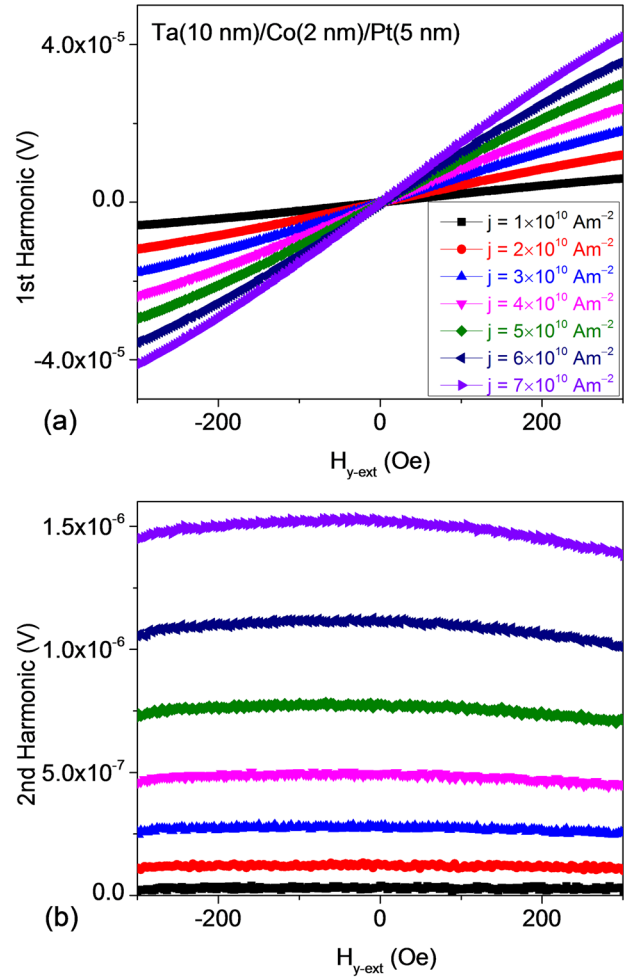


FIG. 2. (a) Measurements of the first harmonic voltages with sweeping in-plane magnetic field for current densities from 1×10^{10} Am $^{-2}$ to 7×10^{10} Am $^{-2}$. The data for each current density are fitted linearly to obtain the slope value, $\frac{\partial V_\omega}{\partial H_{y-ext}}$. (b) Measurements of the second harmonic voltages with sweeping in-plane magnetic field for current densities from 1×10^{10} Am $^{-2}$ to 7×10^{10} Am $^{-2}$. The data for each current density are fitted with parabolic functions to obtain the coefficient of the second order, $\frac{\partial^2 V_{2\omega}}{\partial H_{y-ext}^2}$.

density. The corresponding second harmonic voltages are shown in Fig. 2(b). As expected from Eq. (14), the second harmonic voltage follows a parabolic function of the applied field H_{y-ext} . $\frac{\partial^2 V_{2\omega}}{\partial H_{y-ext}^2}$ can be obtained through fitting the second harmonic curves by parabolic functions. By substituting the values of $\frac{\partial V_\omega}{\partial H_{y-ext}}$ and $\frac{\partial^2 V_{2\omega}}{\partial H_{y-ext}^2}$ obtained from Fig. 2 into Eq. (15), the effective fields for various current densities can be computed. The value of H_{y-ext} is set to 1200 Oe and the contribution of the term $N_y M_s$ is negligible. The effective fields are shown in Fig. 3 as a function of different current densities. In our structure, the field is in the order of 10 Oe for a current density in the order of 10^{10} Am $^{-2}$. The slope of the effective field as a function of current density is about 6 Oe per 10^{11} Am $^{-2}$, which is in the order of the value 5 Oe per 10^{11} Am $^{-2}$ reported in literatures where similar stack with PMA is used.¹¹

B. Thickness dependence

To investigate the effect of the thickness of the HM layer on the field-like term, the Ta layer was varied while

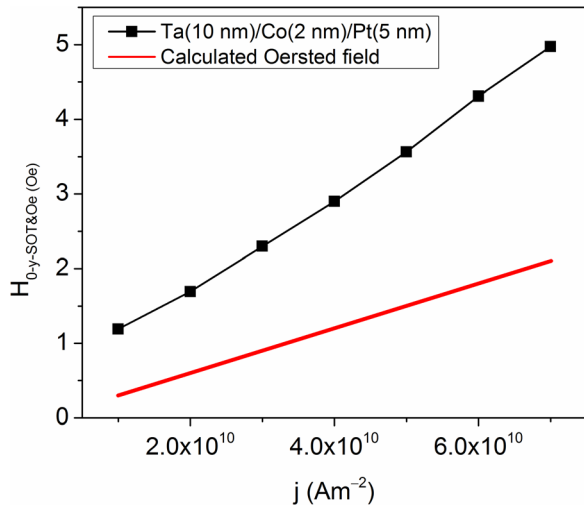


FIG. 3. The obtained effective fields and calculated Oersted field for the sample Ta(10 nm)/Co(2 nm)/Pt(5 nm). The slope of the plotted curve of effective fields is $6 \times 10^{-11} \text{ OeA}^{-1}\text{m}^2$.

keeping the Pt and Co layers fixed. The measurement was repeated on the samples with Ta(x)/Co(2 nm)/Pt(5 nm), with $x = 4 \text{ nm}$ and 8 nm . Shown in Fig. 4 are the representative first and second harmonic voltages. As expected, both

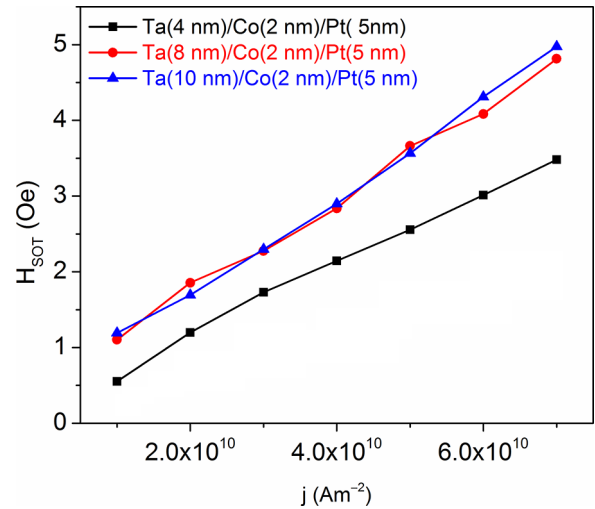


FIG. 5. The obtained field-like term for the samples Ta(4 nm)/Co(2 nm)/Pt(5 nm), Ta(8 nm)/Co(2 nm)/Pt(5 nm), and Ta(10 nm)/Co(2 nm)/Pt(5 nm).

samples display the clear signature of a linear trend for first harmonic signals and a parabolic trend for second harmonic signals. The field-like term is computed for both set of samples and plotted in Fig. 5. For reference, the corresponding field-like term for the sample with Ta = 10 nm is also

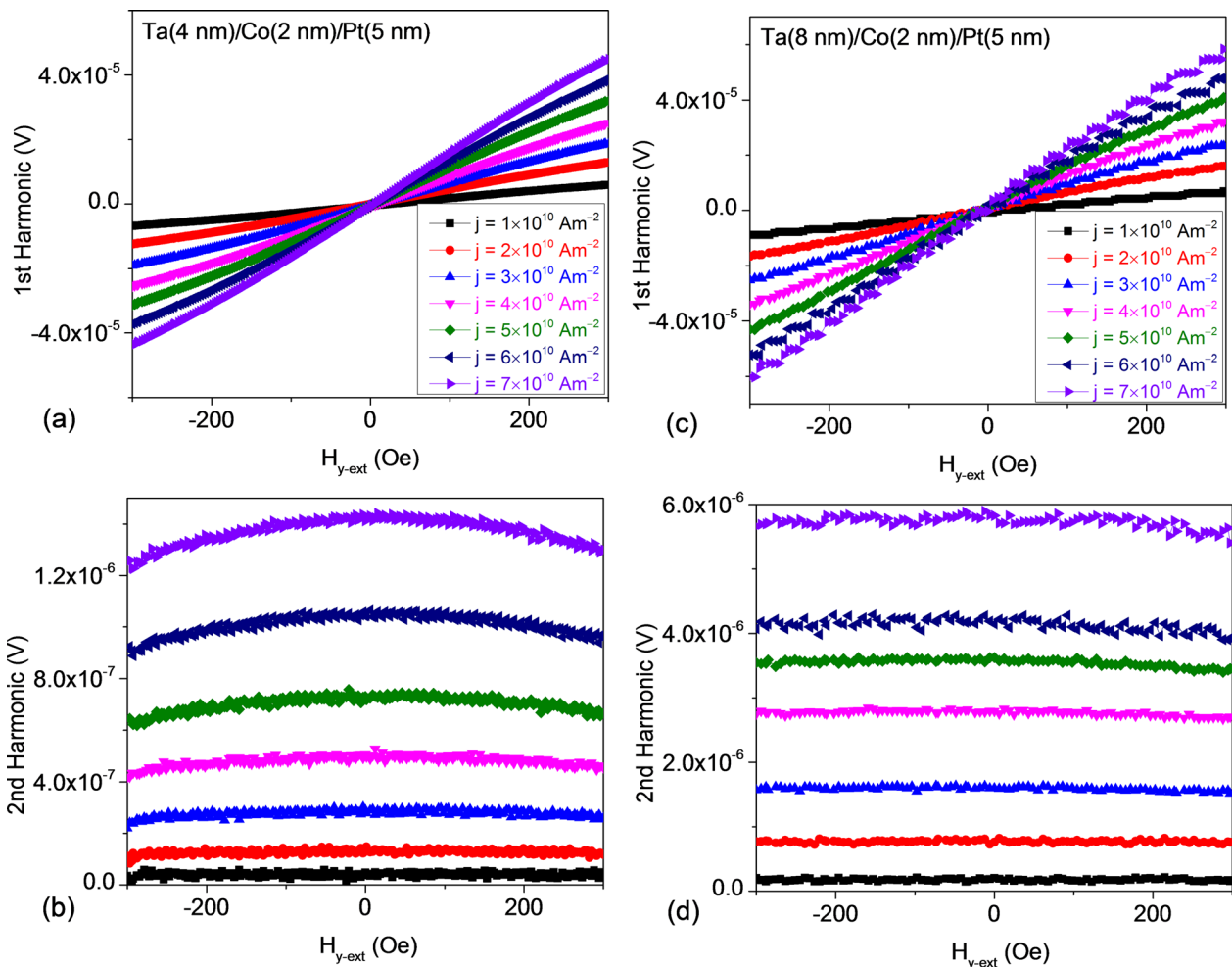


FIG. 4. Measured first and second harmonic voltage (a) and (b) for the sample Ta(4 nm)/Co(2 nm)/Pt(5 nm), and (c) and (d) for the sample Ta(8 nm)/Co(2 nm)/Pt(5 nm).

plotted. The measured field-like term increases with thickness of Ta in our stack configuration.

IV. CONCLUSION

In summary, we have theoretically proposed a method to measure the field-like term of the spin-orbit torque in an in-plane magnetized structure. We have shown that the in-plane transverse field sweep can provide information of the field-like term. Experimental measurements are consistent with the theoretical calculations. The amplitudes of the measured field-like term are in agreement with the results obtained for stack with perpendicular magnetic anisotropy.

ACKNOWLEDGMENTS

This work was supported by the Singapore National Research Foundation, Prime Minister's Office, under a Competitive Research Programme (Non-volatile Magnetic Logic and Memory Integrated Circuit Devices, NRF-CRP9-2011-01), and an Industry-IHL Partnership Program (NRF2015-IIP001-001). The work was also supported by a MOE-AcRF Tier 2 Grant (MOE 2013-T2-2-017). WSL is a

member of the Singapore Spintronics Consortium (SG-SPIN).

- ¹S. S. P. Parkin, M. Hayashi, and L. Thomas, *Science* **320**, 190 (2008).
- ²S. Goolaup, M. Ramu, C. Murapaka, and W. S. Lew, *Sci. Rep.* **5**, 9603 (2015).
- ³A. Thiaville, Y. Nakatani, J. Miltat, and Y. Suzuki, *Europhys. Lett.* **69**, 990 (2005).
- ⁴Z. Li and S. Zhang, *Phys. Rev. Lett.* **92**, 207203 (2004).
- ⁵S. Emori, U. Bauer, S. M. Ahn, E. Martinez, and G. S. D. Beach, *Nat. Mater.* **12**, 611 (2013).
- ⁶K. S. Ryu, L. Thomas, S. H. Yang, and S. Parkin, *Nat. Nanotechnol.* **8**, 527 (2013).
- ⁷I. M. Miron, T. Moore, H. Szambolics, L. D. Buda-Prejbeanu, S. Auffret, B. Rodmacq, S. Pizzini, J. Vogel, M. Bonfim, A. Schuhl, and G. Gaudin, *Nat. Mater.* **10**, 419 (2011).
- ⁸K.-W. Kim, S.-M. Seo, J. Ryu, K.-J. Lee, and H.-W. Lee, *Phys. Rev. B* **85**, 180404 (2012).
- ⁹M. Hayashi, J. Kim, M. Yamanouchi, and H. Ohno, *Phys. Rev. B* **89**, 144425 (2014).
- ¹⁰U. H. Pi, K. W. Kim, J. Y. Bae, S. C. Lee, Y. J. Cho, K. S. Kim, and S. Seo, *Appl. Phys. Lett.* **97**, 162507 (2010).
- ¹¹S. Woo, M. Mann, A. J. Tan, L. Caretta, and G. S. D. Beach, *Appl. Phys. Lett.* **105**, 212404 (2014).
- ¹²H. R. Lee, K. Lee, J. Cho, Y. H. Choi, C. Y. You, M. H. Jung, F. Bonell, Y. Shiota, S. Miwa, and Y. Suzuki, *Sci. Rep.* **4**, 6548 (2014).
- ¹³S. Fukami, T. Anekawa, C. Zhang, and H. Ohno, *Nat. Nanotechnol.* **11**, 621 (2016).